ICFM 10
Adapting to Global Change:
Innovative Approaches to Flood Management and Resilience
May 20-22, 2026 | Western University, London, Ontario, Canada

Historical attribution and future projections of extreme flooding in the transboundary Saint John River Basin

Rajesh R. Shrestha, Alex J. Cannon, Carter Conboy
Climate Research Division, Environment and Climate Change Canada, Victoria, BC, Canada
E-mail: rajesh.shrestha@ec.gc.ca, alex.cannon@ec.gc.ca, carter.conboy@ec.gc.ca

ABSTRACT

The transboundary Saint John River Basin, which covers parts of the provinces of Quebec and New Brunswick in Canada and the state of Maine in the United States, experienced extreme flooding in 2008, 2018, and 2019, with the record-breaking 2018 flood event causing estimated damages of about $75 million in Canada. In this study, we employ a large-scale hydrologic modelling system to characterize these flood events in the context of historical, recent and future climates. Specifically, by conditioning the model on dominant hydroclimatic drivers, we identify anomalously high winter snowpack and spring precipitation as the main drivers of these floods. Furthermore, we show that the events would be even more severe when the two extreme drivers—namely, high winter snowpack and spring precipitation—co-occur. Additionally, by driving the model with an ensemble of statistically downscaled global climate models, we find a small decrease in the intensity of extreme events (e.g. 10–100-year return period) between the historical period (1955–1974) and the recent period (2001–2020). However, projections for the near-future period (2031–2050) suggest an intensification of extreme flooding beyond the most severe historical flood event. Future intensification of flooding occurs despite the projected decline in snowpack, suggesting an increasingly influential role of extreme spring precipitation in driving these floods. Overall, these results underscore the need for adaptation planning to address current and future flood hazards in the region.

KEYWORDS: extreme value analysis**,** future projections, hydroclimatic drivers, hydrological modelling, Saint John River Basin.

1 INTRODUCTION

The transboundary Saint John River, which flows through the provinces of Quebec and New Brunswick in Canada and the state of Maine in the United States within a drainage area of about 55,000 km^2 (Figure 1), is one of the most flood prone rivers in the region. Three large flood events occurred in the basin in 2008, 2018, and 2019, causing extensive property damage and economic losses (Newton and Burrell 2016; Rickard et al. 2025). Specifically, the 2008 flood event was the worst spring flooding in the preceding 35 years in New Brunswick, affecting about 1600 properties and causing damages exceeding Can$23 million (Newton and Burrell 2016; NBGELG 2025). Although the floodwater level in the 2018 event was lower than that of the 2008 event, estimated damages (about Can$75 million) in New Brunswick in 2018 were higher than in 2008 (NBGELG 2025; Rickard et al. 2025). The damages from the 2019 event were lower despite having the peak flow similar to 2018, which was attributed to better flood preparedness (NBGELG 2025). The flood events also caused disruptions to hydropower production from the Saint John River's seven run-of-the-river hydroelectric dams, with floodwater overwhelming the dams' capacity and freely flowing through the spillway, causing substantial financial losses for New Brunswick Power (Web-1). The economic losses and impacts on the communities underscore the need for a better understanding of current and future hazards in the basin.

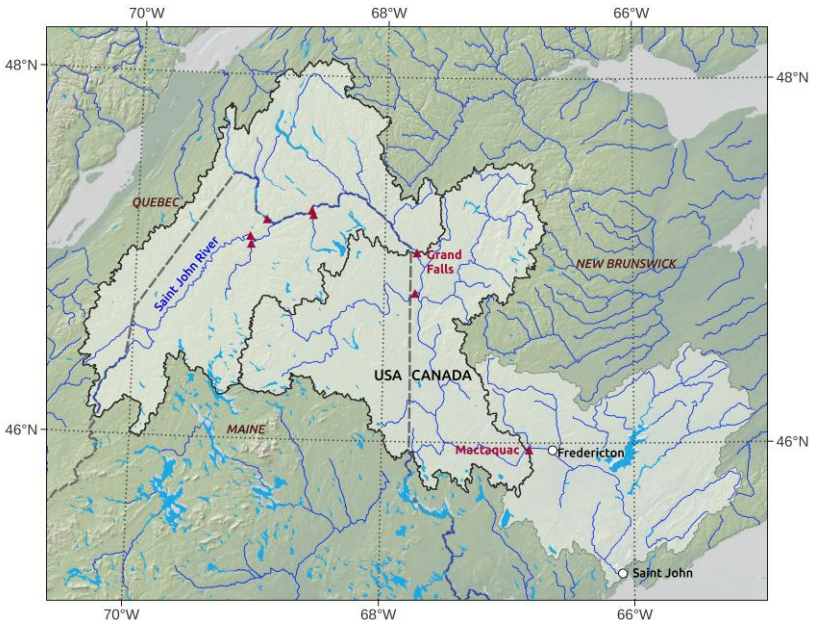

Figure 1. Location map of the Saint John River basin, including the hydrometric stations ▲ used for model calibration.

Floods in the Eastern Maritime region of Canada—where the Saint John River basin is located—primarily occur between March and May, generated by snowmelt, heavy spring precipitation, rain-on-snow events, and augmented by river ice-jamming (Buttle et al. 2016; Newton et al. 2024). Rickard et al. (2025) characterized the main drivers of the three flood events in terms of positive anomalies in winter and spring total precipitation and snow water equivalent (SWE), combined with spring rain-on-snow events. Furthermore, ongoing hydroclimatic changes, especially increasing trends in mean, minimum and maximum air temperature, together with some increases in precipitation, are affecting the magnitude and timing of spring high flows in the region (Caissie and El-Jabi 2024). Additionally, projected increases in precipitation and temperature in the basin can be expected to impact future flood flows and associated risks (El-Jabi et al. 2016; Yousfi et al. 2025).

In this study, we assess current and future flood hazards in the Saint John River basin by using a large-scale hydrological modelling system, the Community Water Model (CWatM) (Burek et al. 2020). Specifically, we drive CWatM with a combination of initial conditions and hydroclimatic drivers conditioned on recent flood events to characterize these events and assess the potential for more extreme events. Furthermore, we drive CWatM with an ensemble of statistically-downscaled Global Climate Models (GCMs) from the Coupled Model Intercomparison Project Phase 6 (Eyring et al. 2016) to assess changes in extreme flows from historical to recent and future climates.

2 METHODS

2.1 Hydrologic Modelling

We set up the CWatM hydrological model (Burek et al. 2020) to simulate historical and future flood response in the Saint John River basin. CWatM is a large-scale, semi-distributed hydrological model developed for global- to regional-scale applications, and the model has been used in previous assessments of historical and future floods (Boulange et al. 2021; Shrestha et al. 2025; Zhao et al. 2025). The model

includes a representation of cold-region processes, including snow accumulation and melt, as well as soil water movement through frozen soil. In this study, we used CWatM version 1.081 with the radiation-restricted degree-day factor snowmelt routine (Erlandsen et al. 2021), which has been modified to account for snow albedo decay (Shrestha et al. 2025).

We employed CWatM at a 5-arcmin resolution, with sub-grid variability in snow and land cover, using static geospatial data provided by the model developers (Web-2). We divided the CWatM setup for the Saint John River basin into upstream and downstream subbasins with outlets at the Grand Falls and Mactaquac hydrometric stations, respectively (Figure 1). We calibrated CWatM parameters for the upstream subbasin by sub-dividing it further into six sub-subbasins, and the downstream subbasin by subdividing it into two sub-subbasins and using flows at the Grand Falls station as inflow. We used flows from each of the six stations in the upstream basin and two stations in the downstream basin as objective functions for calibrating CWatM in a multi-objective framework using the non-dominated sorting genetic algorithm (NSGA-II) (Deb et al. 2002) as implemented in the Python DEAP package (Fortin et al. 2012). Calibration and validation periods consisted of the years 2007-2019 and 1995-2006, respectively.

2.2 Climate Data and Downscaling

We used daily maximum, minimum and mean temperature, total precipitation, downward longwave and shortwave radiation, relative humidity, surface pressure and wind speed from the Canadian Surface Reanalysis (CaSR) version 3.2 (Gasset et al. 2021) as forcing data to calibrate CWatM, and as target data for statistical downscaling. CaSR is a dynamically downscaled observational product based on the Regional Deterministic Reforecast System (RDRS). Gridded precipitation in CaSR is from an offline precipitation analysis using forecast values from RDRS as the background field. CaSR v3.2 has a spatial resolution of ~10 km, spans the period 1980-2024, and covers the entire North American domain. A key advantage of using CaSR for the transboundary Saint John basin is its spatial consistency, i.e. the dataset is not affected by discontinuity at the border.

We used six ensemble members from four CMIP6 GCMs that participated in the High Resolution Model Intercomparison Project (HighResMIP) (Haarsma et al. 2016). The HighResMIP GCMs were selected because of higher spatial resolution (at least 50 km in the atmosphere and 0.25° in the ocean), which reduces the scale of spatial disaggregation between the GCM and target CaSR dataset during downscaling. The selected GCMs span the historical period of 1950-2014 and the future period of 2015-2050 under the Shared Socioeconomic Pathways (SSP) 5-8.5 scenario.

We employed the n-dimensional probability density function transform and multivariate bias correction method (MBCn) (Cannon 2018) to spatially disaggregate and bias-correct GCM outputs to the resolution of the CaSR dataset. This method preserves the multivariate dependence of the target observational data, which is an important consideration for multivariate climate and hydrological extremes. The downscaling was done at the daily time step and includes all variables required for running CWatM, namely: maximum, minimum and mean temperature, total precipitation, downward longwave and shortwave radiation, relative humidity, surface pressure and wind speed.

We forced CWatM with the statistically downscaled GCM outputs and assessed the effect of long-term climate change on extreme flood events. We considered three periods: the historical period of 1955-1974, the recent period of 2001-2020, and the near-future period of 2031-2050 under the SSP5-8.5 scenario, which approximately correspond to 0.25 °C, 1.0 °C, and 2.0 °C of warming, respectively, since the preindustrial period of 1850-1900 (Forster et al. 2023).

2.3 Analyses

To assess the drivers of the flood events of 2008 and 2018, we ran conditional CWatM simulations by combining: i) April 1 initial condition of the flood year with April-August meteorological forcing from 2001-2020, and ii) April 1 initial condition from 2001-2020 with April-August meteorological forcing

from the flood year, excluding the drivers of the remaining flood events in all cases. For example, to assess the role of snowpack on 2008 flooding, we combined April 1 initial condition from 2008 with the 2001-2007, 2009-2017, and 2020 April-August meteorological drivers. Similarly, to assess the role of spring conditions on the 2008 flood, we combined the 2008 April-August meteorological drivers with April 1 initial condition from 2001-2007, 2009-2017 and 2020.

We analyzed extreme value statistics of annual maximum flows for each of the 20-year historical, recent and future periods, by assuming stationarity over each period, but non-stationarity across the three periods. Specifically, for each 20-year period, we combined all annual maximum flow values from the six-member GCM ensemble driven CWatM simulations and fitted the Generalized Extreme Value (GEV) distribution for the combined sample size of 120. The GEV distributions were fitted using the L-moments parameter estimation (Hosking 1990) (Hosking and Wallis, 1993), as implemented in the R extRemes package (Gilleland 2024).

3 RESULTS

3.1 CWatM calibration/validation

In this paper, we focus on the results for the Saint John River at Grand Falls station. The performance of the calibrated CWatM model generally indicates a good ability to represent the dynamics of streamflow hydrograph, with the Kling–Gupta efficiency (KGE) of 0.85 and 0.80 for the calibration and validation periods, respectively. However, the model had difficulty in replicating the peak flow magnitudes of some flood events, e.g. the 2019 event (Figure 2a). These discrepancies arise from a number of sources of uncertainties, including: i) forcing data, e.g. representativeness of precipitation and temperature in the CaSR reanalysis data; ii) observed streamflow data, e.g. estimated flows based on water levels, especially when affected by river ice; and iii) model structure, i.e. representation of underlying physical processes in the CWatM model. Nevertheless, the comparison of the quantiles of the observed versus simulated annual peak flows indicates a reasonable ability of the model to reproduce the distribution of extremes (Figure 2b), except for the maximum of all events.

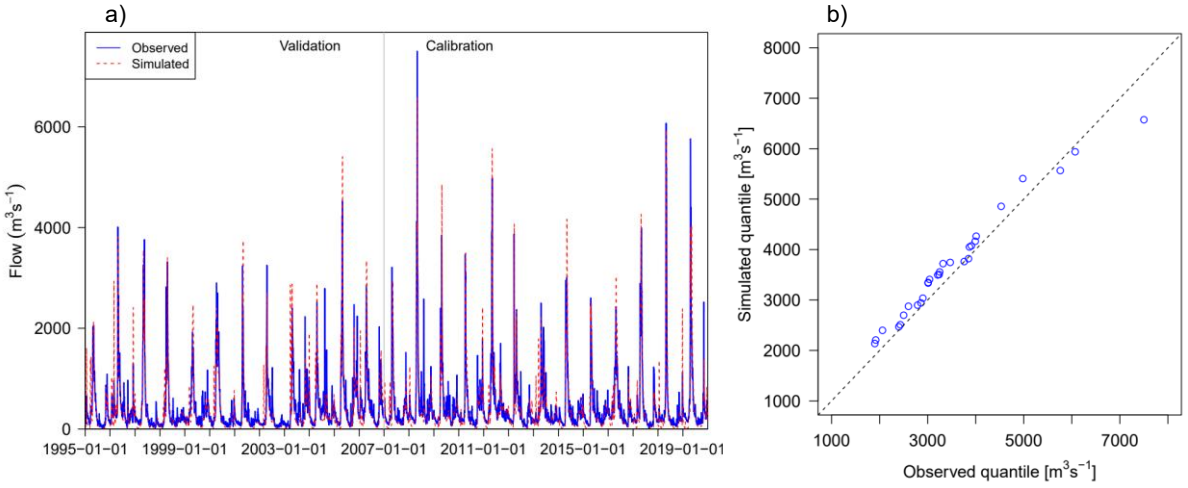

Figure 2: Observed vs. CWatM simulated discharge at the Saint John River at Grand Falls station: a) calibration (2007-2019) and validation (1995-2006) results; b) quantile–quantile plot of the distribution of observed vs. simulated annual peak flows over both calibration and validation period.

3.2 Effects of the drivers on the 2008 and 2018 flood events

The 2008 and 2018 flood events occurred between April 23 and May 12 (Rickard et al. 2025), and based on CWatM simulations, 2008 and 2018 April 1 SWE values are about 86% and 30% above 2001-2020 mean value, with the 2008 April 1 SWE value being highest over the entire period. April precipitation values were more variable, with the 2008 and 2018 values at about 8% and 35% of the 2001-2020 means, respectively.

The combined simulations i) and ii), corresponding to the drivers of the 2008 flood, revealed contrasting responses (Figure 3). Specifically, the simulations i) conditioned on the 2008 April 1 initial condition, show a substantial shift in the distribution of maximum flows, with the maximum of maximums about 29% higher, and 5 of 17 simulated flows higher than the 2008 event. This illustrates the potential for larger floods when the 2008 snowpack co-occurs with higher spring precipitation than in 2008. Furthermore, the large shift in the distribution of flows between 2001-2020 and simulations i), illustrate the dominant effect of the anomalously large snowpack on the 2008 flood event. The simulations ii), conditioned on the 2008 April-August meteorological drivers, resulted in a lower maximum of maximums and smaller shift in the distribution. This suggests limited effect of the spring meteorological conditions on the 2008 flood event.

The simulations i) and ii), corresponding to the 2018 flood event, both show maximum of maximums approximately equal to the 2018 event. Hence, the combinations of drivers of the 2018 flood event with 2001-2020 hydroclimatic conditions, excluding those from the 2008 and 2019 events, do not lead to a larger flood than in 2018. However, the differences in shifts in the distribution of maximum flows in the two sets of simulations indicate their differing influences on the 2018 flood event. Specifically, the smaller shift in simulations i) suggests smaller effect of the April 1 snowpack, while the larger shift in simulations ii) suggests larger effect of the spring meteorological drivers.

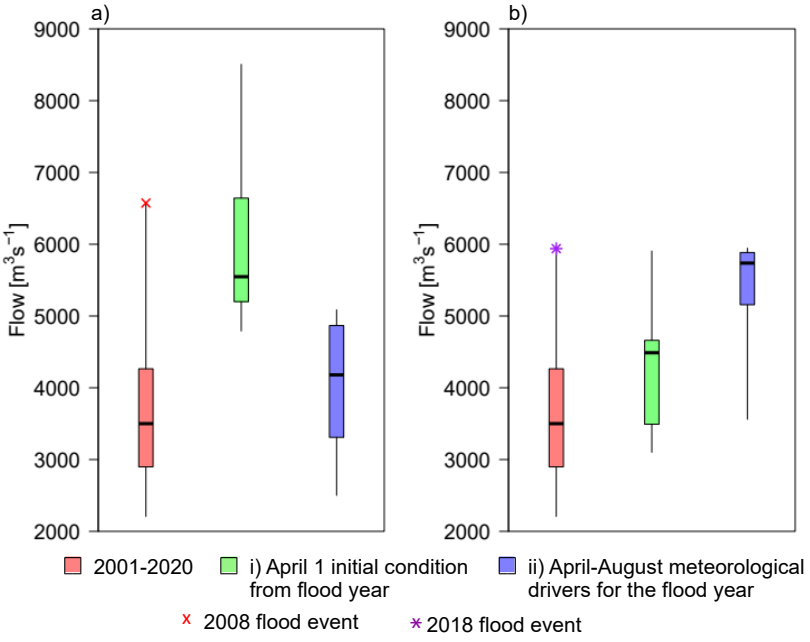

Figure 3: 2001-2020 simulated discharge together with simulations conditioned on: i) April 1 initial condition and, ii) April-August meteorological drivers corresponding to a) 2008 flood event and b) 2018 flood event. Boxplots depict interquartile ranges and whiskers depict maximum and minimum. The simulations i) and ii) for a) excludes the forcings from the 2018 and 2019 events and simulations i) and ii) for b) excludes forcings from the 2008 and 2019 events.

3.3 Comparison with historical and future simulations

The comparison of simulated April 1 SWE over the historical (1955-1974), recent (2001-2020) and near-future (2031-2050) periods generally shows successive declines over the three periods, indicating the influence of warming temperatures on snowpack storage in the basin. The decreases in snowpack occur despite increases in precipitation between each period, suggesting a warmer temperature-driven increase in the rainfall fraction of total precipitation. In general, maximum flows increase progressively from historical to recent to near-future periods. However, the maximum of the six-member ensemble for the recent period is lower than that of the historical period, indicating the variability across the ensembles used.

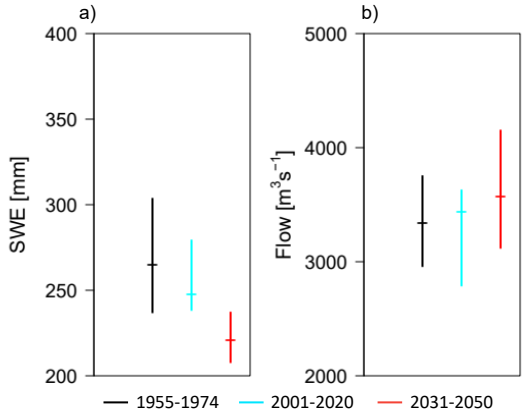

Figure 4: Comparison of simulated a) April 1 SWE and b) maximum flow over the historical (1955-1974), recent (2001-2020) and near-future (2031-2050) periods. The ranges show maximum, median and minimum values obtained from the 20-year means of each of the 6-member GCM driven CWatM simulations.

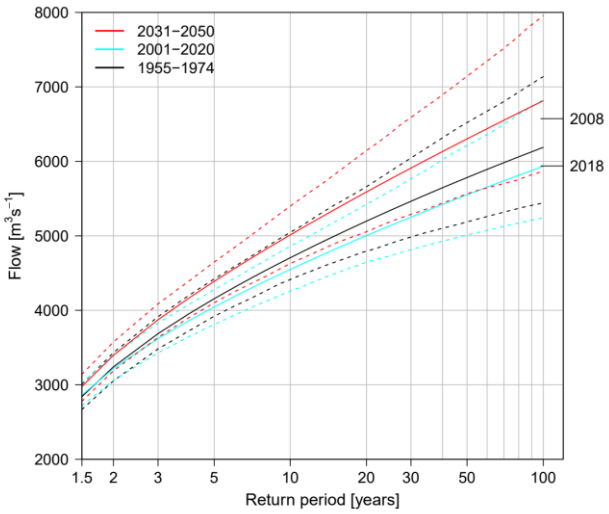

Figure 5. Flood frequency curves obtained by fitting the GEV distribution on the annual maximum flows. All GCM ensemble members are combined for the GEV fitting, and the dashed lines show the 95% confidence intervals of the fitted distribution. The years on the right axis indicate flows for two highest-recorded historical flood events.

We also analyzed the changes in flood frequencies across the three periods by fitting the GEV distribution to the annual maximum flows from all GCM ensemble members combined (Figure 5). The comparison of results between the historical and recent periods shows similar flows for floods of smaller

return periods (e.g. 1.5- and 2-year flood events). However, the curves diverge at higher return periods, which is consistent with the lower maximum for the recent period when the 20-year means of the GCM-driven simulations are compared (Figure 4). The projected flows for the 2031-2050 near-future period are higher than both the historical and recent periods at all return periods. Consequently, the return period of the 2018 flood event decreases from about 101-year to 31-year between the recent and near-future periods, respectively. Likewise, the return period of the 2008 flood event decreases from about 354-year to 72-year between the two periods, respectively. Hence, the model simulations suggest an intensification of extreme flooding in the near-future period, with flood events beyond the highest historical flood event of 2008 becoming increasingly common. Furthermore, future intensification of flooding occurs despite the projected decline in snowpack, suggesting an increasingly influential role of extreme spring precipitation in driving these floods.

4 CONCLUSION

This study provides an evaluation of historical, recent and future changes in flood hazard in the Saint John River basin in the context of the 2008, 2018 and 2019 flood events. We employ a large-scale hydrologic modelling system CWatM to characterize these flood events. Our evaluation identified the anomalously high snowpack as the main drivers of the 2008 flood event, and both high winter snowpack and spring precipitation as the drivers of the 2018 event. Furthermore, the results show the potential for flood events larger than the observed, under the compounding influence of high snowpack (such as in 2008), and high spring precipitation. Our evaluation also showed a general decrease in snowpack depth but an increase in maximum flows progressively from historical (1955-1974) to recent (2001-2020) to near-future (2031-2050) periods. In terms of the return periods of extreme maximum flow, the projections show small increases between the historical and recent periods, but larger decreases between the recent and future periods. This suggests future intensification of extreme flooding beyond the most severe historical flood events. Overall, these results underscore the need for an adaptation planning against current and future flood hazards in the region.

REFERENCES

Boulange J, Hanasaki N, Satoh Y, et al (2021) Validity of estimating flood and drought characteristics under equilibrium climates from transient simulations. Environ Res Lett 16:104028. https://doi.org/10.1088/1748-9326/ac27cc

Burek P, Satoh Y, Kahil T, et al (2020) Development of the Community Water Model (CWatM v1.04) – a high-resolution hydrological model for global and regional assessment of integrated water resources management. Geoscientific Model Development 13:3267–3298. https://doi.org/10.5194/gmd-13-3267-2020

Buttle JM, Allen DM, Caissie D, et al (2016) Flood processes in Canada: Regional and special aspects. Can Water Resour J 41:7–30. https://doi.org/10.1080/07011784.2015.1131629

Caissie D, El-Jabi N (2024) Hydrometeorological trends under a changing climate in New Brunswick Part 1 of 2: Final Report

Cannon AJ (2018) Multivariate quantile mapping bias correction: an N-dimensional probability density function transform for climate model simulations of multiple variables. Clim Dyn 50:31–49. https://doi.org/10.1007/s00382-017-3580-6

Deb K, Pratap A, Agarwal S, Meyarivan T (2002) A fast and elitist multiobjective genetic algorithm: NSGA-II. IEEE Transactions on Evolutionary Computation 6:182–197. https://doi.org/10.1109/4235.996017

El-Jabi N, Caissie D, Turkkan N (2016) Flood analysis and flood projections under climate change in New Brunswick. Canadian Water Resources Journal / Revue canadienne des ressources hydriques 41:319–330. https://doi.org/10.1080/07011784.2015.1071205

Erlandsen HB, Beldring S, Eisner S, et al (2021) Constraining the HBV model for robust water balance assessments in a cold climate. Hydrology Research 52:356–372. https://doi.org/10.2166/nh.2021.132

Eyring V, Bony S, Meehl GA, et al (2016) Overview of the Coupled Model Intercomparison Project Phase 6 (CMIP6) experimental design and organization. Geoscientific Model Development 9:1937–1958. https://doi.org/10.5194/gmd-9-1937-2016

Forster PM, Smith CJ, Walsh T, et al (2023) Indicators of Global Climate Change 2022: annual update of large-scale indicators of the state of the climate system and human influence. Earth System Science Data 15:2295–2327. https://doi.org/10.5194/essd-15-2295-2023

Fortin F-A, De Rainville F-M, Gardner M-AG, et al (2012) DEAP: evolutionary algorithms made easy. J Mach Learn Res 13:2171–2175

Gasset N, Fortin V, Dimitrijevic M, et al (2021) A 10 km North American precipitation and land-surface reanalysis based on the GEM atmospheric model. Hydrology and Earth System Sciences 25:4917–4945. https://doi.org/10.5194/hess-25-4917-2021

Gilleland E (2024) extRemes: Extreme Value Analysis

Haarsma RJ, Roberts MJ, Vidale PL, et al (2016) High Resolution Model Intercomparison Project (HighResMIP v1.0) for CMIP6. Geoscientific Model Development 9:4185–4208. https://doi.org/10.5194/gmd-9-4185-2016

Hosking JRM (1990) L-Moments: Analysis and Estimation of Distributions Using Linear Combinations of Order Statistics. Journal of the Royal Statistical Society: Series B (Methodological) 52:105–124. https://doi.org/10.1111/j.2517-6161.1990.tb01775.x

NBGELG (2025) Flood History Database, Saint John River (Watershed). https://www.elgegl.gnb.ca/0001/en/Flood/Search?LocationName=Saint+John+River+%28watershed%29. Accessed 3 Dec 2025

Newton B, Beltaos S, Burrell BC (2024) Ice regimes, ice jams, and a changing hydroclimate, Saint John (Wolastoq) River, New Brunswick, Canada. Nat Hazards 120:12613–12642. https://doi.org/10.1007/s11069-024-06736-5

Newton B, Burrell BC (2016) The April–May 2008 flood event in the Saint John River Basin: Causes, assessment and damages. Canadian Water Resources Journal / Revue canadienne des ressources hydriques 41:118–128. https://doi.org/10.1080/07011784.2015.1009950

Rickard LJ, Déry SJ, Stewart RE, Thériault JM (2025) Meteorologically Related Factors Leading to the 2008, 2018, and 2019 Major Spring Floods in the Transboundary Saint John River (Wolastoq) Basin. Journal of Hydrometeorology 26:201–220. https://doi.org/10.1175/JHM-D-24-0032.1

Shrestha RR, Cannon AJ, Hoffman S, et al (2025) Benchmarking historical performance and future projections from a large-scale hydrologic model with a watershed hydrologic model. Hydrology and Earth System Sciences 29:2881–2900. https://doi.org/10.5194/hess-29-2881-2025

Yousfi N, El Adlouni S, Gachon P (2025) Non-stationary and multivariate spring floods estimation of the Saint John River (eastern Canada). Stoch Environ Res Risk Assess 39:3063–3084. https://doi.org/10.1007/s00477-025-03008-x

Zhao F, Nie N, Liu Y, et al (2025) Benefits of Calibrating a Global Hydrological Model for Regional Analyses of Flood and Drought Projections: A Case Study of the Yangtze River Basin. Water Resources Research 61:e2024WR037153. https://doi.org/10.1029/2024WR037153

Web sites

Web-1 https://www.cbc.ca/news/canada/new-brunswick/mactaquac-dam-flood-2018-1.4948716, accessed 5 December 2025

Web-2 ftp://rcwatm:Water1090@ftp.iiasa.ac.at/, accessed 3 December 2025